SANDIA REPORT

SAND2010-6724
Unlimited Release
Printed September 2010

Use of Metal Organic Fluors for Spectral Discrimination of Neutrons and Gammas

F. Patrick Doty, Mark D. Allendorf, Patrick L. Feng

Prepared by
Sandia National Laboratories
Albuquerque, New Mexico 87185 and Livermore, California 94550

Sandia National Laboratories is a multi-program laboratory managed and operated by Sandia Corporation, a wholly owned subsidiary of Lockheed Martin Corporation, for the U.S. Department of Energy's National Nuclear Security Administration under contract DE-AC04-94AL85000.

Issued by Sandia National Laboratories, operated for the United States Department of Energy by Sandia Corporation.

Available to DOE and DOE contractors from
U.S. Department of Energy
Office of Scientific and Technical Information
P.O. Box 62
Oak Ridge, TN 37831

Telephone: (865) 576-8401
Facsimile: (865) 576-5728
E-Mail: reports@adonis.osti.gov
Online ordering: http://www.osti.gov/bridge

Available to the public from
U.S. Department of Commerce
National Technical Information Service
5285 Port Royal Rd.
Springfield, VA 22161

Telephone: (800) 553-6847
Facsimile: (703) 605-6900
E-Mail: orders@ntis.fedworld.gov
Online order: http://www.ntis.gov/help/ordermethods.asp?loc=7-4-0#online

SAND2010-6724
Unlimited Release
Printed September 2010

Use of Metal Organic Fluors for Spectral Discrimination of Neutrons and Gammas

F. P. Doty, Mark D. Allendorf, Patrick L. Feng
Department Names
Sandia National Laboratories
P.O. Box 0969
Livermore, CA, MS9402

Abstract

A new method for spectral shape discrimination (SSD) of fast neutrons and gamma rays has been investigated. Gammas interfere with neutron detection, making efficient discrimination necessary for practical applications. Pulse shape discrimination (PSD) in liquid organic scintillators is currently the most effective means of gamma rejection. The hazardous liquids, restrictions on volume, and the need for fast timing are drawbacks to traditional PSD scintillators.

In this project we investigated harvesting excited triplet states to increase scintillation yield and provide distinct spectral signatures for gammas and neutrons. Our novel approach relies on metal-organic phosphors to convert a portion of the energy normally lost to the scintillation process into useful luminescence with sub-microsecond lifetimes. The approach enables independent control over delayed luminescence wavelength, intensity, and timing for the first time. We demonstrated that organic scintillators, including plastics, nanoporous framework materials, and oil-based liquids can be engineered for both PSD and SSD.

ACKNOWLEDGMENTS

Many members of the work force contributed their expertise in material synthesis and characterization. In particular Dr. Andy Vance provided polymer materials, Dr. Scott Meek synthesized organic molecules required for some MOFs used here, Dr. John Perry assisted in MOF synthesis, and Dr. Raghu Bhakta provided assistance with MOF infiltration methods. Ion beam induced luminescence and cathodoluminescence were acquired by Janelle Branson, and Michael Smith, respectively. Special thanks are due to Dr. Pin Yang for his diligent handing of the cathodoluminescence studies.

CONTENTS

FIGURES

TABLES

NOMENCLATURE

AIBN	Azobisisobutyronitrile (radical polymerization reaction initiator)
CDF	Cumulative probability distribution function
CL	Cathodoluminescence
DUT-6	Dresden University of Technology # 6: Zn_4O(2,6-NDC)(benzenetribenzoate)$_{4/3}$(DEF)$_{16}$(H_2O)$_{9/2}$
FOM	Figure of merit
IBIL	Ion beam induced luminescence
Ir(ppy)$_3$	Tris[2-phenylpyridinato-C2,N]iridium(III)
Ir(ppy-F_2)$_3$	Tris[2-(4,6-difluorophenyl)pyridinato-C2,N]iridium(III)
Ir(quin)$_3$	Tris[1-phenylisoquinoline-C2,N]iridium(III)
Ir(thio)$_3$	Tris[2-(benzo[b]thiophen-2-yl)pyridinato-C3,N]iridium(III)
IRMOF	Isoreticular MOF, conforms to Zn_4O-L_3
IRMOF-10	L = 4,4'-biphenyldicarboxylate
ISC	Intersystem crossing
-L	Ligand (e.g. phenylisoquinoline; see Ir(quin)$_3$)
LET	Linear energy transfer
M_{PSD}	Figure of merit for pulse shape discrimination
M_{SSD}	Figure of merit for spectral shape discrimination
MLCT	Metal-ligand charge transfer
MOF	Metal Organic Framework
MOF-4	Zn_2(benzenetricarboxylate)(NO_3)(EtOH)$_3$
NDC	Naphthalenedicarboxylate, fluorescent linker used in DUT-6
PL	Photoluminescence
PMT	Photomultiplier tube
POPOP	1-4,bis-2-(5-Phenyloxazolyl)-benzene (Secondary fluor in combination with PPO)
PPO	2,5-Diphenyloxazole (Primary fluor for scintillating solutions)
PSD	Pulse shape discrimination
PtOEP	Platinum octaethylporphyrin
PVK	Poly(9-vinylcarbazole)
RHT	MOFs comprising rhombicuboctahedral, tetrahedral, and cuboctahedral cages
S	Singlet state
S0	Singlet ground state
S1	Lowest excited singlet state
SOC	Spin-orbit coupling
SSD	Spectral shape discrimination
T	Triplet state
T1	Lowest excited triplet state
TCSPC	Time correlated single photon counting

1. INTRODUCTION

New organic scintillators are needed for particle discrimination. Traditional liquid scintillators are hazardous and do not perform well in large volumes. Crystal structures of organic molecules demonstrated for PSD are low symmetry and therefore always optically anisotropic, requiring growth of single crystals for their use as scintillators. Existing plastic scintillators have so far not exhibited adequate triplet transport for traditional PSD. Therefore a new approach to particle discrimination is a worthy pursuit.

Upon particle ionization, organic scintillators relax rapidly and nonradiatively to the lowest available excited states before emitting scintillation light. By spin multiplicity, these intermediate states comprise 25% singlet (S1) and 75% triplet (T1) excitation. Since the direct T1 to S0 transition is spin-forbidden, most of the triplet excitation is lost to the scintillation process, with a minor component being converted to S1 through T-T annihilation, giving rise to delayed fluorescence. This intrinsic delayed signal is found to be less sensitive to quenching at high excitation density (dE/dx) than the fast component, which is the basis of traditional pulse shape discrimination (PSD). Excited triplet states that do not undergo T-T annihilation are a pure loss in organic scintillators, which accounts for their low luminosity. Conversely, these states represent a large reservoir of unused energy which could be harvested to improve scintillation signals.

In this project we investigated harvesting excited triplet states to increase scintillation yield and provide distinct spectral signatures for gammas and neutrons. The approach exploits a well-known heavy-atom effect, spin-orbit coupling, to provide prompt radiative transitions for excited triplet states, producing delayed extrinsic luminescence for particle discrimination. This effect was previously used to identify the triplet adsorption state in stilbene[1] and, subsequently to create bright, fast-emitting phosphors for organic light-emitting diodes[2], resulting in a near theoretical 4-fold increase in efficiency. It was recently shown to increase light yield in plastic scintillators[3]. Third-row transition metals such as iridium, osmium, and platinum, induce strong spin-orbit coupling; and efficient mixing between the singlet metal-to-ligand charge transfer (MLCT) states and the ligand-based states are achieved, resulting in emission quantum efficiencies approaching 100%.

Since plastics loaded with high concentrations of metal-organic fluors have already been demonstrated, and MOF loading with heavy metals has been demonstrated to levels in excess of the saturation levels in plastics, there is clear potential to build triplet-harvesting sites within a low-cost isotropic host.

2. APPROACH

Our approach to engineering organic scintillators exploits spin orbit coupling in metal-organic complexes to break the quantum spin restriction for triplet relaxation, providing a prompt radiative pathway to convert the triplet energy reservoir into useful luminescence. As mentioned above, this approach was successfully used to quadruple the efficiency of organic LEDs in recent years, and a substantial literature supported our analysis that it would significantly increase scintillation yield. Furthermore, the emission can be tuned over the entire visible range, enabling scintillators to be designed with separable triplet and singlet spectra, separating the singlet from triplet emission by wavelength, as well as arrival time. As with prior PSD scintillators, these distinct spectral components were predicted to be sensitive to particle type due to greater dE/dx quenching of the faster singlet emission.

The approach is illustrated in Figure 1, which shows schematic energy levels for a generic organic scintillator. Scintillation is unlike photoluminescence in that the excitation does not simply promote electrons into an excited state manifold, but removes electrons from their parent

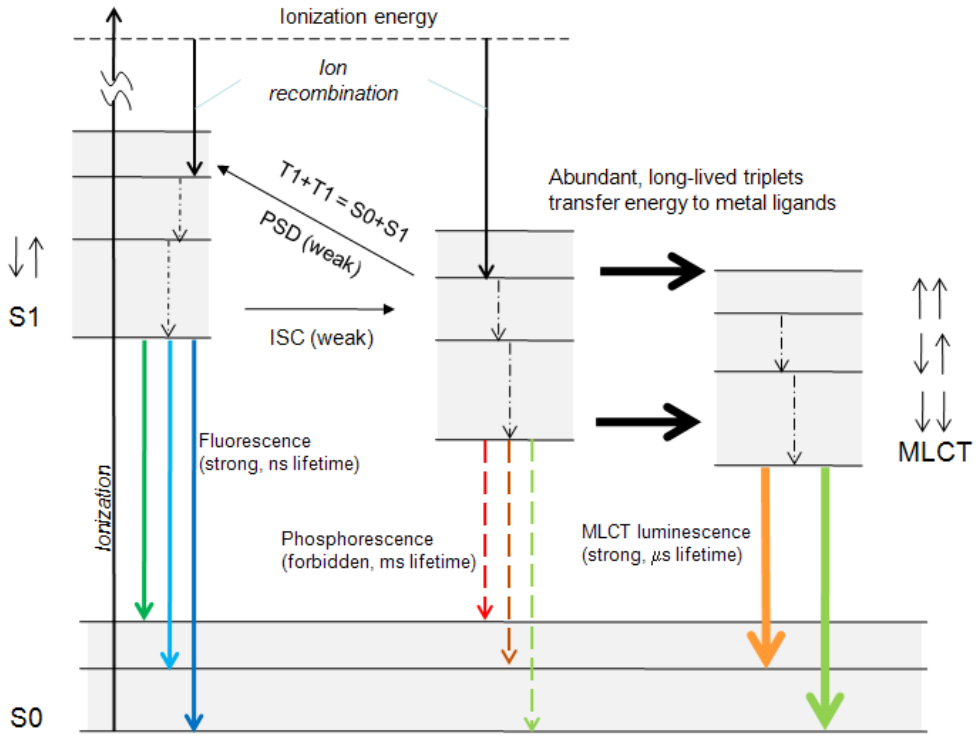

Figure 1. New approach to scintillator engineering

molecules. Therefore ion recombination is required to populate the excited states from above, resulting in direct population of excited triplets as well as singlets. Since there are three times as many triplet states, only ¼ of the initial excitation will produce fast fluorescence.

The intrinsic delayed emission is a weak fluorescence from slow re-population of S1 following T-T annihilation, as seen on the left in Figure 1. This process is not very efficient, and relies on mobile triplet states, resulting in a complex, long-tailed kinetic-diffusion time dependence[4]. Because it is transport mediated, only materials with high triplet mobility (certain molecular crystals or aromatic liquids) exhibit this kind of delayed emission with enough intensity to be useful for pulse shape discrimination.

By contrast, the new approach relies on efficient triplet energy transfer to metal-ligand charge transfer (MLCT) states introduced through an extrinsic heavy metal-organic complex, illustrated on the right in Figure 1. Spin-orbit coupling with the metal drastically increases the transition rate, resulting in exponential phosphorescent emission on a time scale commensurate with traditional PSD. This new, extrinsic delayed luminescence has intensity proportional to the concentration of the MLCT, and can thus be controlled through doping.

Many commercially available platinum metal complexes exhibit a high degree of MLCT, which correlates with effective triplet harvesting. The complexes used for this project (Figure 2) were purchased from Sigma-Aldrich, Inc**.** These fluors exhibit a range of wavelengths enabling separable spectral features for intrinsic and extrinsic emissions.

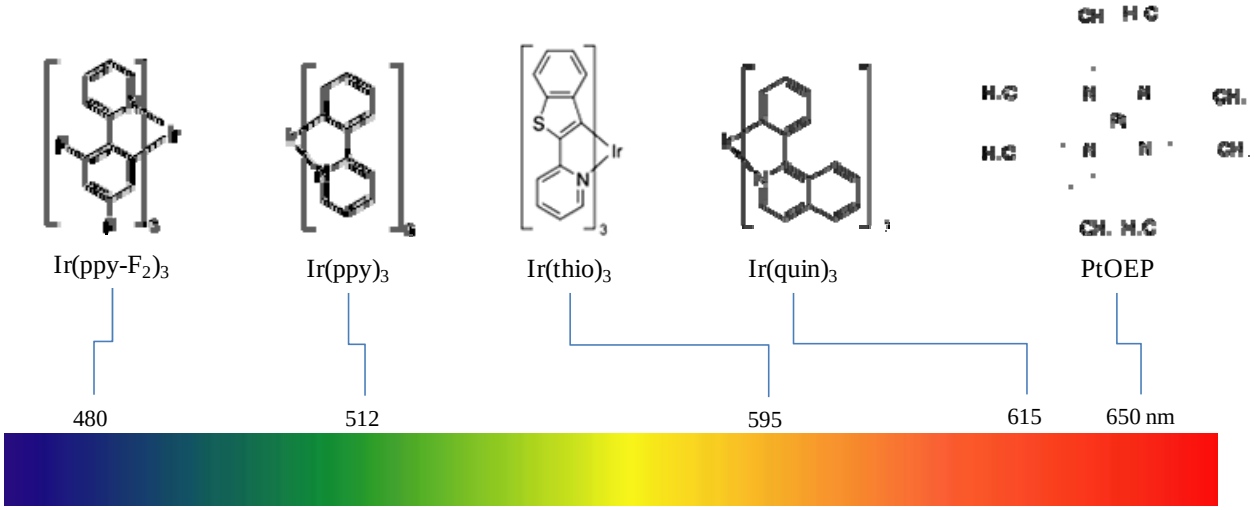

Figure 2. Metal-organic phosphors used in this work

These fluors were introduced into a variety of host materials to form new composite scintillators, as described in the next section.

3. MATERIAL SYNTHESIS

Procedures used for host material syntheses and introduction of commercial metal-organic phosphors are outlined below. A number of the complexes shown in Figure 2 were introduced into each host; a complete list of material combinations tested is given in Table 1, page 17.

3.1 Plastic Scintillator (PVK):

Initial PVK samples were prepared by drop casting from chlorobenzene solutions onto microscope slides. Two stock solutions were prepared, containing 1.) low-molecular weight Poly(9-vinylcarbazole) obtained from Sigma-Aldrich, and 2.) low concentrations of $Ir(ppy)_3$. Small portions of the metal-organic solution were added to ten ml aliquots of the polymer solution for drop-casting. Bulk iridium and platinum doped plastic scintillators were also prepared via in-situ polymerization of the monomer components or through dissolution. Polymerization was accomplished according to established methods, employing AIBN as a radical initiator.

3.2 IRMOF-10:Solvent Infiltration Method

IRMOF-10 was prepared via an adaptation of the previously reported method reported.[5] Briefly, zinc nitrate hexahydrate, $Zn(NO_3)_2 \cdot 6H_2O$ (0.186 g, 0.625 mmol) and 4,4'-biphenyldicarboxylic acid, 4,4'-$BPDCH_2$ (0.030 g, 0.124 mmol), were dissolved in 50 mL of N,N-diethylformamide and placed in a glass bottle. The vessel was sealed and heated at a constant rate (1.5^o C/min) to 85^o C for 15 hours and then cooled to ambient temperature at a rate of 2^o C/min. The resultant sample (48%) was washed with N,N-dimethylformamide (3x15 mL), followed by chloroform (3x15 mL). The crystals were then evacuated for 3 hours at 50 mTorr, transferred to a N_2 glovebox, and mixed with a chloroform solution (5 mL) of $Ir(ppy)_3$ (0.8 mg, $1.22 \cdot 10^{-3}$ mmol), $Ir(ppy\text{-}F_2)_3$ (1.0 mg, $1.31 \cdot 10^{-3}$ mmol), $Ir(thio)_3$ (1.1 mg, $1.34 \cdot 10^{-3}$ mmol), $Ir(quin)_3$ (1.1 mg, $1.37 \cdot 10^{-3}$ mmol), or Pt(OEP) (1.0 mg, $1.37 \cdot 10^{-3}$ mmol)). After 8 hours, the infiltrated crystals were washed with fresh chloroform (5x15 mL). ICP-OES on the above (IRMOF-10 + $Ir(ppy)_3$) preparation indicates an Iridium metal loading ratio of 0.99% (w/w).

3.3 DUT-6 and MOF-4: Ship-in-bottle Infiltration Method

DUT-6 was prepared via a procedure similar to the previously reported method.[6] Important modifications include the rigorous removal of O_2 from the reaction mixture, use of a lower temperature, and the in-situ 'ship-in-bottle' incorporation of iridium or platinum heavy-metal complexes. Fluorescent 2,6-naphthalenedicarboxylic acid (NDC) (0.034 g, 0.16 mmol) and 1,3,5-tris(4-carboxyphenyl)benzene (0.108 g, 0.246 mmol) were dissolved in N,N-diethylformamide (20 mL) and mixed with a DEF solution (2 mL) of zinc nitrate hexahydrate, $Zn(NO_3)_2 \cdot 6H_2O$ (0.117 g, 0.393 mmol). $Ir(thio)_3$ (1.1 mg, $1.34 \cdot 10^{-3}$ mmol), $Ir(quin)_3$ (1.1 mg,

$1.37 \cdot 10^{-3}$ mmol), or Pt(OEP) (1.0 mg, $1.37 \cdot 10^{-3}$ mmol)) were added, followed by rigorous O_2-degassing using N_2. The sample bottle was then sealed and heated to 80°C for 10 hours, resulting in respective yellow, orange, or red colored octahedral crystals (1mm x 1mm x 1mm) of infiltrated DUT-6. The crystals were washed with p-Xylenes (3x15mL) or chloroform (3x15mL) and soaked overnight to remove surface impurities. No luminescence was observed in the final soak solutions, indicating no diffusion of the infiltrated molecules out of the MOF pores. The loading ratios may also be varied by changing the initial concentration of phosphorescent Iridium or Platinum complexes in the reaction mixture, as evidenced by smooth variations of the relative peak intensities in the photoluminescence emission spectra.

MOF-4 was prepared via a procedure similar to the previously reported method.[7] Important modifications include the addition of a fluorescent guest molecule such as 1,4-naphthalenedicarboxylic acid or 4,4'-stilbenedicarboxylic acid, rigorous removal of O_2 from the reaction mixture, and the addition of phosphorescent iridium or platinum heavy-metal complexes. In a representative synthesis, 1,4-naphthalenedicarboxylic acid (0.034 g, 0.160 mmol) and trimesic acid (0.035 g, 0.167 mmol) were dissolved in 4 mL of N,N-diethylformamide and added to a DEF (2 mL) solution of zinc nitrate hexahydrate, $Zn(NO_3)_2 \cdot 6H_2O$ (0.256 g, 0.860 mmol) and $Ir(ppy)_3$ (0.8 mg, $1.22 \cdot 10^{-3}$ mmol), $Ir(ppy\text{-}F_2)_3$ (1.0 mg, $1.31 \cdot 10^{-3}$ mmol), $Ir(thio)_3$ (1.1 mg, $1.34 \cdot 10^{-3}$ mmol), $Ir(quin)_3$ (1.1 mg, $1.37 \cdot 10^{-3}$ mmol), or Pt(OEP) (1.0 mg, $1.37 \cdot 10^{-3}$ mmol)). The mixture was rigorously O_2-degassed using N_2 and heated to 80°C for 10 hours, resulting in colored clear polyhedral crystals (1mm x 0.8mm x 0.8mm) of infiltrated MOF-4. The crystals were washed with p-Xylenes (3x15mL) or chloroform (3x15mL) and soaked overnight to remove surface impurities. No luminescence was observed in the final soak solutions, indicating no diffusion of the infiltrated molecules out of the MOF pores. The loading ratios may also be varied by changing the initial concentration of phosphorescent Iridium or Platinum complexes in the reaction mixture, as evidenced by smooth variations of the relative peak intensities in the photoluminescence emission spectra. The incorporation of fluorescent guest molecules in the MOF-4 pores was performed to render the non-emissive crystalline framework luminescent, and was accomplished by direct ship-in-bottle addition of the organic fluors and phosphorescent metal complexes to the reaction mixture.

3.4 Mineral Oil-based scintillator:

2,5-diphenyloxazole (PPO), (10 mg, 0.045 mmol) and Ir(quin)3 (0.4 mg, mmol) were dissolved in 1 mL $CHCl_3$ and subsequently added to 20 mL of mineral oil. The mixture was then rigorously degassed using N_2 to remove dissolved O_2. Alternate mixtures containing other heavy-metal phosphors, or differing primary or secondary fluor combinations, may be devised. The phosphors include but are not limited to $Ir(ppy)_3$, $Ir(ppy\text{-}F_2)_3$, $Ir(quin)_3$, $Ir(thio)_3$, and Pt(OEP). Primary or secondary fluors include but are not limited to p-terphenyl, PPO, POPOP, anthracene, naphthalene, diphenylanthracene, and trans-stilbene.

4. RESULTS

Representative results for PVK and two MOF-based materials are given in this section. A complete list of materials tested is given in Table 1 on page 17; and in all cases the resulting hybrid materials showed intrinsic fluorescence from the host and sub-μs to μs extrinsic phosphorescence from the dopant. The timing characteristics of each state were determined using PL excitation, while the dE/dx dependence of steady-state spectra were observed from particle excitation in proton and electron beam systems at Sandia.

The principles of the approach are illustrated below in Figure 3, which shows the cubic MOF DUT-6 crystals infiltrated with $Ir(quin)_3$. This MOF has large cage structures capable of accommodating phosphorescent complexes of Ir and Pt used in our studies. The spectrum shows the intrinsic ligand-based luminescence near 380 nm due to the isolated naphthalene moieties in framework, and extrinsic phosphorescence of the complex centered near 600 nm. The separate luminescence images were made using 290 nm photo excitation and 450 nm high- and low edge pass filters. Several of these MOF composites were synthesized by "ship in bottle" and are listed as MOF category 1 in the table on page 17.

The choices of NDC and $Ir(quin)_3$ make obvious that the triplet and singlet states are non-interacting under UV excitation, and can easily be separated using optical filters. The easy substitution of host and guest luminophores to either differentiate (for SSD) or match (for PSD) wavelengths depending on application make this an attractive approach for rational design of new scintillator materials and signatures.

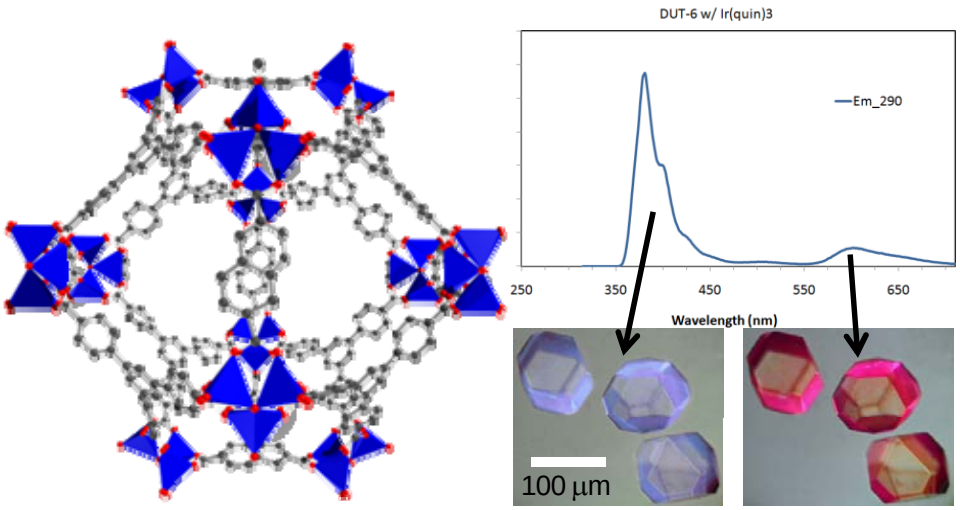

Figure 3. DUT6 infiltrated with $Ir(quin)_3$. Tetrahedral clusters in the structure represent Zn coordination to oxygen atoms on the framework ligands. The intrinsic blue-UV luminescence is from naphthalene in the framework, the red is extrinsic from $Ir(quin)_3$.

4.1 Poly(vinylcarbazole)

The first materials tested for radioluminescence were PVK films drop-cast from solutions as described above, with low concentrations of $Ir(ppy)_3$. To prevent complete transfer of singlet to MLCT excitation by intersystem crossing in this system, it was found that concentrations well below 1% by weight are required. The initial dilute films were drop cast and tested for PL in a nitrogen-purged atmosphere to prevent oxygen quenching of the triplet luminescence. It was found that air quenching is fully reversible in seconds, and that subsequent of steady-state spectra taken under vacuum were stable immediately after pump down.

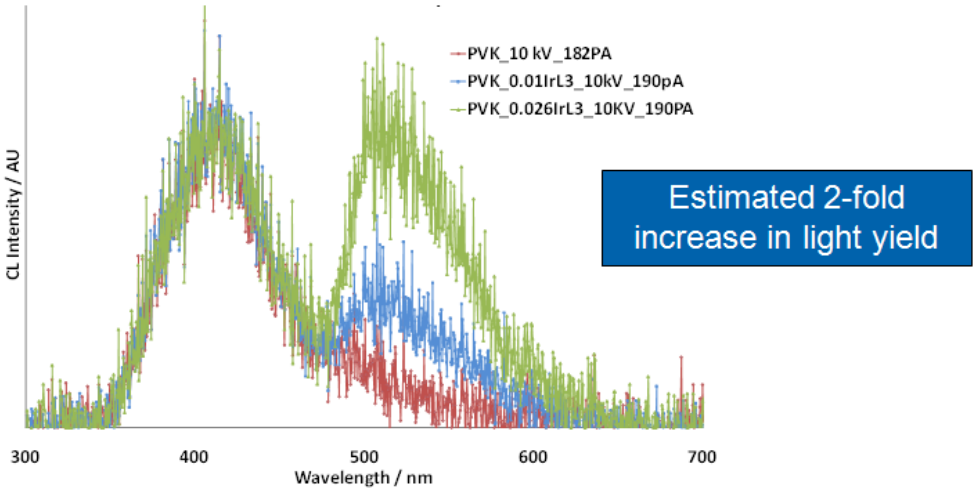

Figure 4. Increased radioluminosity of doped PVK (L = phenylpyridine).

Figure 4 shows cathodoluminescence (CL) of neat PVK, as well as PVK films doped with 0.01 and 0.026 weight per cent $Ir(ppy)_3$. The spectra were acquired for 30 second under nearly identical beam conditions of 10kV accelerating voltage and 182-190 pA probe current. The relative intensities of intrinsic blue (410 nm) and extrinsic green (520 nm) luminescence indicate a two-fold increase in the luminosity is achieved for 0.026% addition of the complex, which corresponds to just 75 ppm iridium metal on a molar basis.

The timing characteristics of the intrinsic and extrinsic components of the doped films were determined by time correlated single photon counting (TCSPC) using PL excitation at 337 nm. Using a fast Si photodetector to generate a start pulse from the N2 laser, and band bass filters centered on 410 and 520 nm to select the emission wavelengths, the delay times for single photons detected by a poorly coupled PMT recorded. The timing distributions thus determined are plotted in **Error! Reference source not found.Error! Reference source not found.**. The decay curves are very similar for the two doping levels used, showing fast fluorescence from the host PVK, which fits to a double exponential, (0.91 EXP[-t/10ns] + 0.09 EXP[-t/ 40 ns]), and single exponential (1.0 EXP[-t/550ns]) for the extrinsic luminescence.

The quenching behavior of these luminescence features was investigated using a 3 MeV ion beam induced luminescence (IBIL) to produce high dE/dx protons, and a 30 keV electron beam to produce relatively low dE/dx cathodoluminescence (CL). The first direct evidence of spectral shape discrimination is seen in Figure 6. These spectra were necessarily acquired under very different conditions in tow different systems, yet the long-wavelength phosphorescence features appear identical. The curves were therefore normalized to match in the tail region, to compare the relative intensities of the host luminescence for the two particle types.

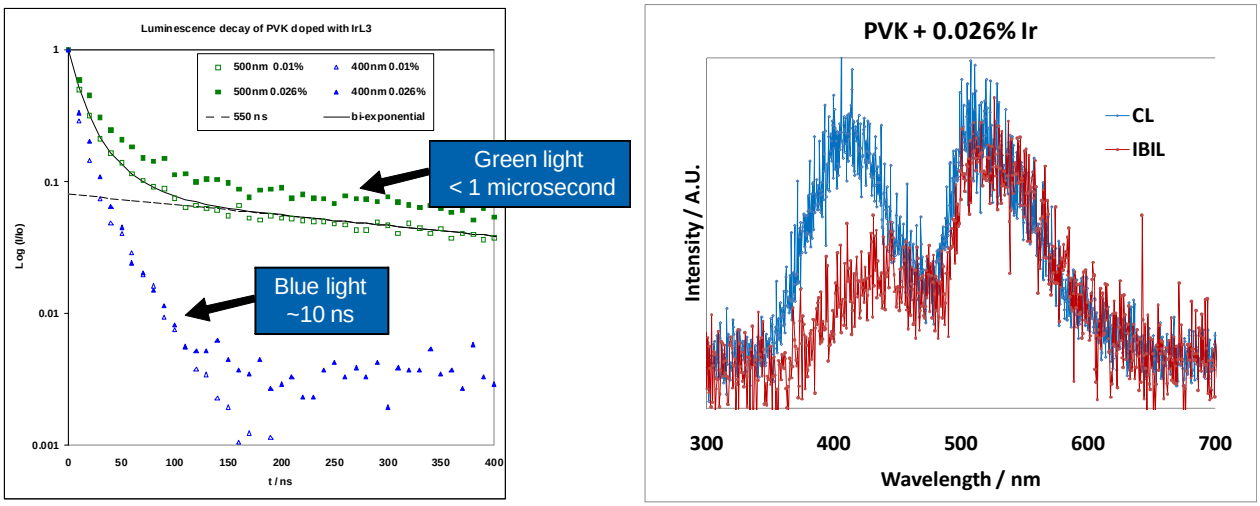

Figure 5. Host and guest photo luminescence decay in PVK by TCSPC.

Figure 6. SSD in PVK. Extrinsic luminescence intensity is insensitive to dE/dx.

The results are qualitatively similar to traditional PSD, in that the fluorescence is substantially quenched by MeV proton excitation relative to the delayed triplet-derived luminescence. However, the intensity of the delayed phosphorescence is much greater than the delayed fluorescence used in PSD, which will dramatically improve photon statistics low energies, decreasing the threshold for practical particle discrimination. This effect may enable gains in sensitive volumes, and should apply to both timing- and spectral based discrimination.

It is significant that the intensity of the delayed signal observed in doped PVK is much greater than the delayed fluorescence in traditional PSD liquids and molecular single crystal, enabling practical particle discrimination in PVK plastic scintillator for the first time. This system is analyzed in more detail in section 5. SSD Figure of merit 18.

4.2 Metal organic framework materials

Metal organic frameworks are crystalline materials consisting of metal clusters linked by coordinating organic groups, that can be predicted through an understanding of the geometric nets accessible to particular metal-linker combinations.[8,9,10] The predictability of framework topology, wide variety of fluorescent linker moieties, and nanometer sized pores capable of accommodating non-interacting guest molecules make MOFs a very attractive system for ‘‘crystal engineering’’, rational design of new scintillation materials.[11] Sandia currently has multiple ongoing projects synthesizing new MOFs, which were made available to this project .

The first data showing spectral discrimination in a MOF are shown in Figure 7. This is an example of MOF composite category 2, doped by solvent infiltration of the phosphorescent complex. The host material, IRMOF-10, comprises fluorescent biphenyl- dicarboxylate linkers in a cubic framework with pores just large enough to accommodate the $Ir(quin)_3$ complex. As was seen for the PVK doped with $Ir(ppy)_3$, separable spectral features are observed, and the fast fluorescence is quenched to a greater extent than the delayed extrinsic phosphorescence under high dE/dx excitation.

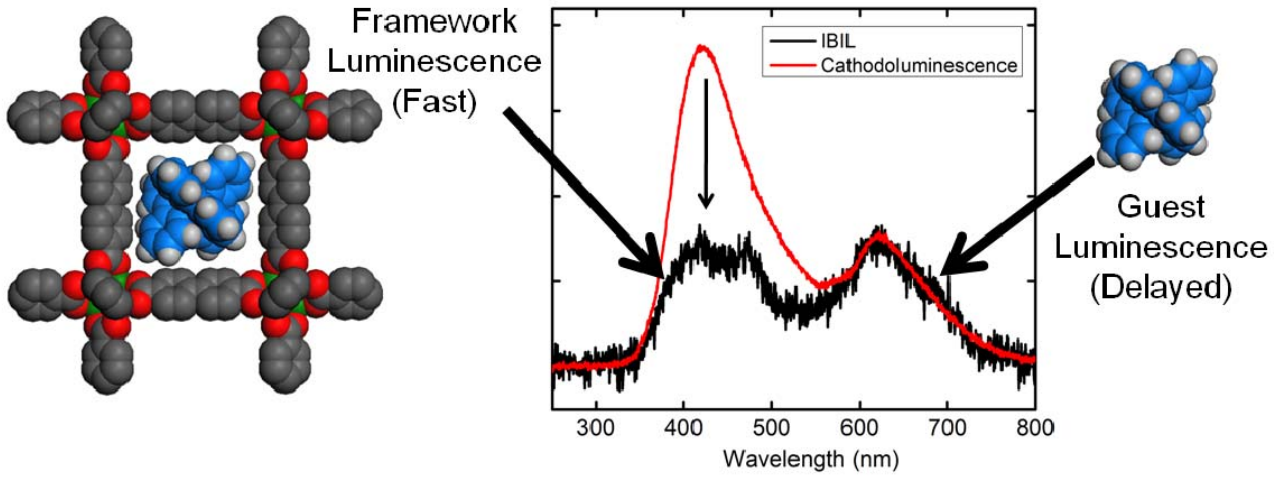

Figure 7. Demonstration of SSD in IRMOF10 infiltrated with Tris[1-phenylisoquinolinato] Iridium(III). The framework fluorescence dominating the cathodoluminescence is substantially quenched when excited by MeV protons.

The timing distributions for these emission features were determined under photo excitation as seen in **Error! Reference source not found.**Figure 8. Again, as with the polymer, the intrinsic signal is several orders of magnitude faster than the extrinsic phosphorescence of the complex, which should enable efficient pulse shape discrimination of neutrons and gammas.

It should be noted that the emission wavelengths of linkers and dopants were arbitrarily chosen to observe large separation of the spectral features, for unambiguous identification of the radiative transitions. Optimal materials for SSD and PSD will have emissions matched to efficient photon detectors such as PMTs.

Error! Reference source not found.

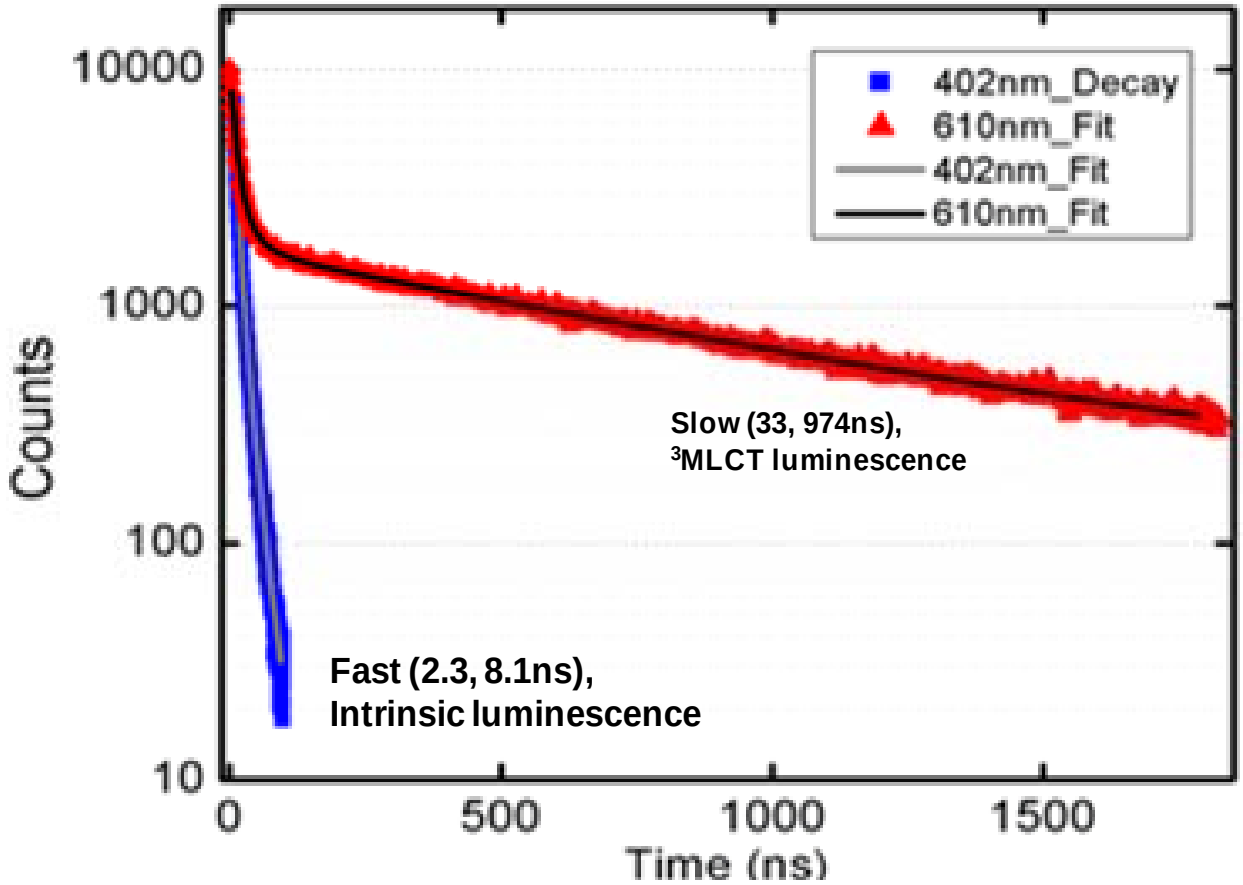

Figure 8. TCSPC distributions of fluorescence and phosphorescence features from IRMOF10 infiltrated with Tris[1-phenylisoquinolinato] Iridium(III).

Another way to engineer the spectral emission is to use a non-luminescent MOF as a host for both fluorescent and phosphorescent guest complexes. Examples of this approach, listed under MOF category 3 in Table 1, are based on MOF-4 co-infiltrated with naphthalene dicarboxylic acid and various phosphors.

4.3 Oil based compositions

Mineral oil is a nonhazardous base for high H/C organic scintillators. Although outside the original scope for the project, several oil-based compositions were compounded, to show the generality of the approach. As with plastic and MOF based composites, these composition exhibited separable spectral and TCSPC timing features under photo excitation.

Table 1. Compositions demonstrated

Plastic-Based Materials

1. PVK + 0.010% $Ir(ppy)_3$ (SSD verified via steady-state CL and IBIL)
2. PVK + 0.026% $Ir(ppy)_3$ (SSD verified via steady-state CL and IBIL)
3. PVK + 0.026% $Ir(ppy\text{-}F2)_3$
4. PVK + 0.026% $Ir(quin)_3$
5. PVK + 0.026% $Ir(thio)_3$
6. PVK + 0.050% PtOEP

MOF-Based Materials

Category 1: DUT-6. (Synthesized via **ship-in-bottle** synthesis: intact truncated octahedral crystals.) [Note: Ship-in-bottle synthesis was effective presumably due to very large pore volume. However, solvent infiltration into the evacuated neat MOF was not effective due to small pore opening. This may be an advantage for preventing the ship-in-bottle Iridium complexes from diffusing out of the large pores]

1. DUT-6 w/$Ir(quin)_3$.
2. DUT-6 w/$Ir(thio)_3$

Category 2: IRMOF-10. (Synthesized via **solvent infiltration** into evacuated MOF: opaque cubic crystals)

1. IRMOF-10 w/ $Ir(ppy)_3$ (ICP analysis reveals 0.99% Iridium by weight)
2. IRMOF-10 w/$Ir(ppy\text{-}F2)_3$
3. IRMOF-10 w/$Ir(quin)_3$ (SSD verified via steady-state CL and IBIL)
4. IRMOF-10 w/$Ir(thio)_3$ (SSD verified via steady-state CL and IBIL)
5. IRMOF-10 w/PtOEP

Category 3: MOF-4 (Synthesized via **ship-in-bottle** synthesis: intact truncated octahedral crystals.) [Note: the MOF framework has no intrinsic luminescence; fluorescence is imparted by guest naphthalenedicarboxylic acid molecules (or other luminescent groups)]

1. MOF-4 w/ 1,4-naphthalenedicarboxylic acid (primary singlet fluor) + Ir(quin)3.
2. MOF-4 w/1,4-naphthalenedicarboxylic acid (primary singlet fluor) + Ir(thio)3.

Category 4: RHT-1. (Synthesized via **ship-in-bottle and solvent infiltration** into evacuated MOF: intact octahedral crystals and opaque octahedra, respectively)

1. RHT-1 w/$Ir(ppy)_3$.
2. RHT-1 w/$Ir(thio)_3$.
3. RHT-1 w/$Ir(quin)_3$.
4. RHT-1 w/PtOEP

Oil-based Liquid Scintillator

1. 5 mg POPOP + 20 mL Mineral Oil + 0.4 mg $Ir(quin)_3$ + 2 mL $CHCl_3$
2. 10 mg PPO + 20 mL Mineral Oil + 0.4 mg $Ir(quin)_3$ + 1 mL $CHCl_3$

5. SSD FIGURE OF MERIT

The key idea for SSD is to apply wavelength-dependent detection of the luminescent signals to achieve specificity. We have analyzed the efficacy of this method for neutron and gamma detection, and proposed a new spectral shape discrimination figure of merit, M_{SSD}, which is statistically equivalent to the well known pulse-shape discrimination figure of merit M_{PSD}.

A Mathematica Notebook was created to analyze electron and proton pulses from the experimental CL and IBIL spectra. The analysis determines SSD FOM using a simulation procedure exactly analogous to experimental determination of PSD FOM, as explained by Horrocks[12], choosing a dichroic wavelength instead of a timing threshold to bin events. This is achieved by first fitting the experimental spectra, integrating the fits, and normalizing to obtain cumulative probability distribution functions (CDFs) for the two types of events (analogous to Horrocks, Fig. 8). These CDFs are used to randomly generate pulses of different sizes corresponding to photons detected for each kind of event (electron or proton excitation). An example histogram showing two simulated 1000-photon pulses is shown in Figure 8.

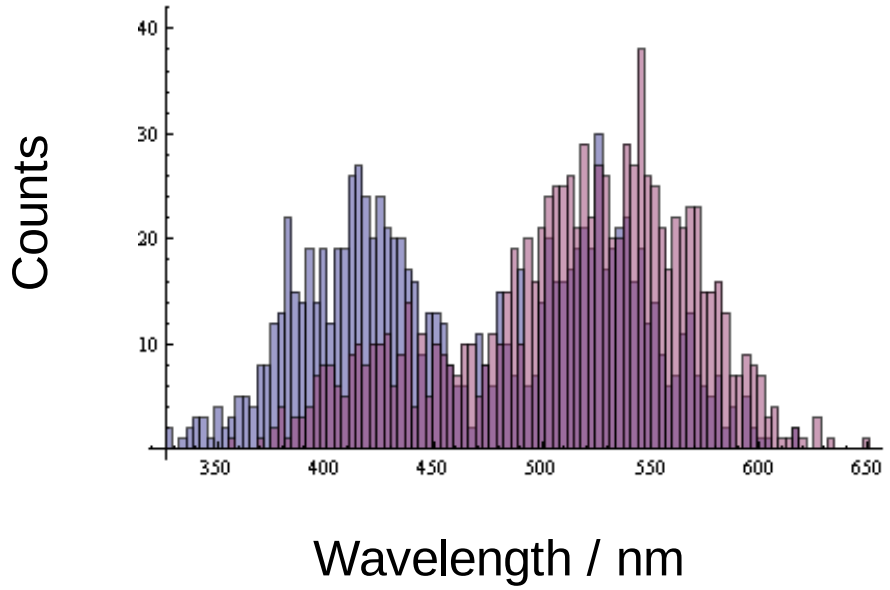

Figure 8 Simulated 1000-photon pulses from doped PVK for (pink) IBIL and (blue) CL.

In PSD, PMT pulses are integrated in real time on a capacitance, and the crossing time at an arbitrary constant fraction of the integrated pulse is recorded. In this way an optimum fraction is determined, giving optimum timing bins for resolution of the electron and proton pulses. In analogy, simulated SSD pulses are numerically integrated with respect to wavelength. In this way the optimum dichroic wavelength is determined. Typical results of this process are shown in Figure 9.

For the particular histogram shown in Figure 9, a 40% fraction is assumed, which corresponds to a dichroic wavelength of 450 nm. The figure of merit is defined as the difference in the means of the distributions divided by the sum of their FWHMs (about 4.0 for this dichroic wavelength and

number of photons detected). The lower plot in Figure 9 shows the FOM calculated in this way as a function of dichroic wavelength, for different numbers of photons detected. The analysis shows that PVK with 0.026% $Ir(ppy)_3$ has an optimal dichroic wavelength of 465 nm.

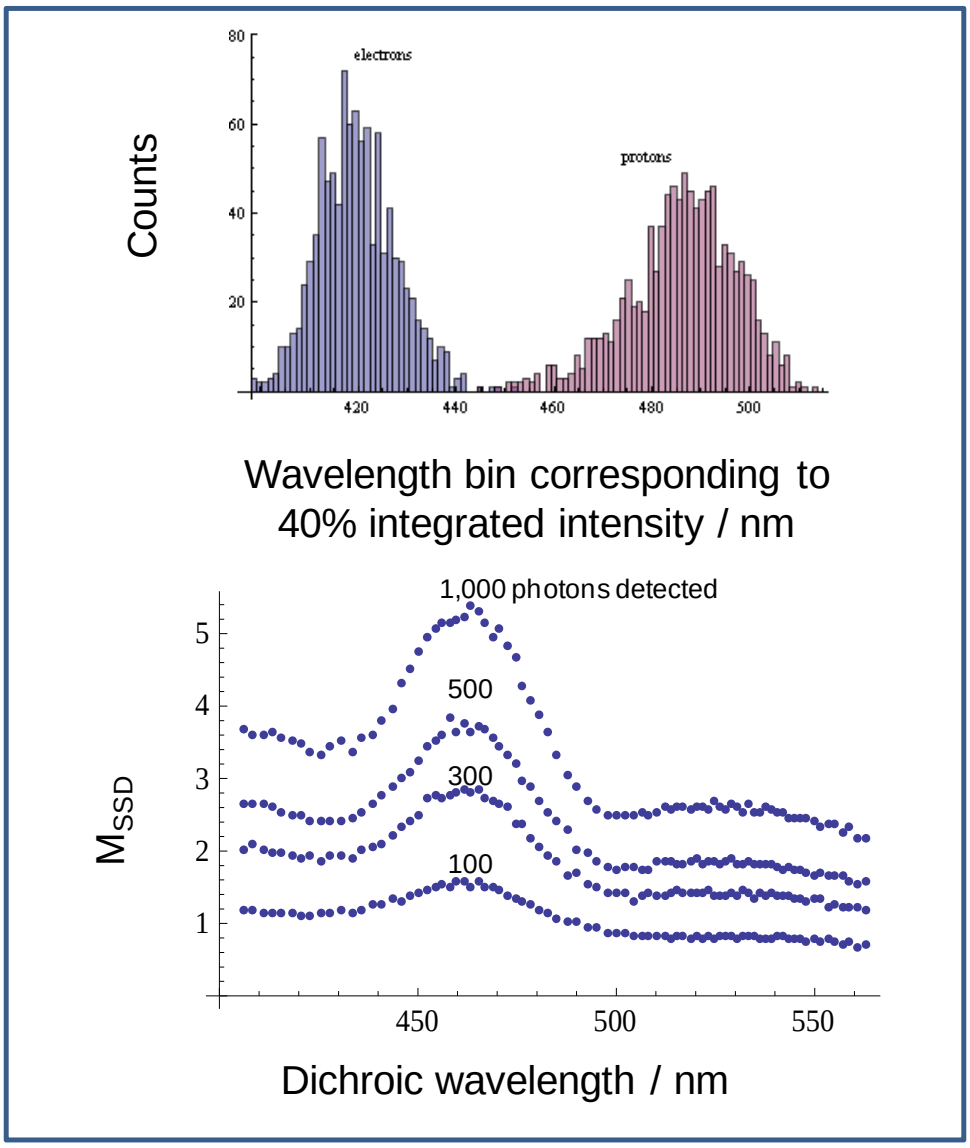

Figure 9. SSD figure of merit versus dichroic wavelength for PVK w/0.026% $Ir(ppy)_3$. Upper plot shows 1000-event histograms for wavelength of 40% fraction integrated (corresponding to 450 nm dichroic wavelength) for 1000-photon pulses from fast proton (pink) and electron (blue) excitation. The lower plot shows calculated FOM [(difference in means)/(sum of FWHMs)] versus dichroic wavelength for different size pulses.

The analysis shows M_{SSD} does not depend critically on wavelength, and the optimum wavelength does not depend on pulse height. To compare M_{SSD} and M_{PSD} magnitudes directly requires only an accurate determination of the luminosity, and scaling of the spectral distributions with the sensitivity of the photodetector.

6. APPLICATIONS

Both PSD and SSD materials can be engineered through the approach detailed in this report. Timing-based particle discrimination is well known, and dramatically improved PSD materials are anticipated using our approach. In particular, plastic scintillators with high intensity delayed exponential luminescence should make plastics capable of efficient PSD for the first time.

Spectral shape discrimination is a new approach, with the potential advantages of relaxed timing requirements and larger sensitive volumes. Wavelength-dependent detection may employ dichroic filters, wavelength dispersive optics, multilayer or tandem detectors, photodiode arrays, etc., to separately sense photons emitted in different spectral regions. For example, efficient light collection can be achieved using non-absorptive dichroic filters, as illustrated in Figure 10.

Note that M_{SSD} does not depend critically on wavelength for the prototype plastic scintillator of Figure 9, remaining $\geq$ 4.0 over the range 450 – 480 nm; thus un-sharpness and angular dependence of dichroic filter transitions will not strongly influence gamma rejection by SSD. Furthermore, the predicted optimum dichroic wavelength is independent of the signal strength.

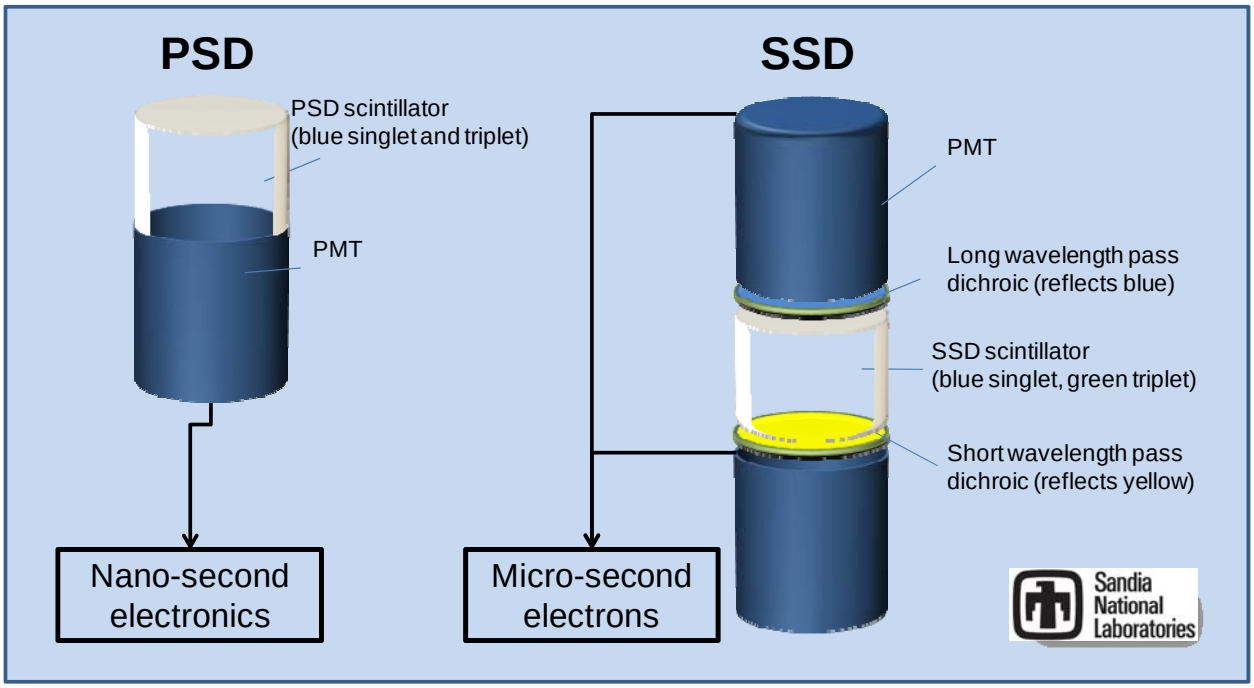

Figure 10. Systems for particle discrimination

7. Conclusions

New luminescent materials were found to emit distinct spectra upon ionization with energetic protons and electrons. The materials are fast organic scintillators doped with phosphorescent heavy metal complexes to produce a secondary delayed luminescence which is less sensitive to ionization quenching than the host luminescence. By varying organic ligands coordinating with the heavy metal, it is possible to tune the emission spectrum and lifetime of the extrinsic state. Using this approach, crystalline, plastic, and liquid scintillators were shown to exhibit emission wavelength based particle discrimination.

Because the wavelength, intensity and timing of the extrinsic luminescence can be independently controlled, this approach enables engineering of improved scintillators for both PSD and SSD.

[Blank page following section.]

8. REFERENCES

[1] Dyck, R. H.; McClure, D. S."Ultraviolet spectra of stilbene, p-monohalogen stilbenes, and azobenzene and the trans to cis photoisomerization process," J. Chem. Phys. 36, 2326 (1962).

[2] Thompson, M."The evolution of organometallic complexes in organic light-emitting diodes," MRS Bull., 32, 694 (2007).

[3] I. H. Campbell_ and B. K. Crone, "Efficient plastic scintillators utilizing phosphorescent dopants", Applied Phys. Lett., 90, 012117 (2007).

[4] G. Laustriat, *Molecular Crystals and Liquid Crystals*, 4, 127-145 (1968).

[5] Eddaoudi, M.; Kim, J.; Rosi, N.; Vodak, D.; Wachter, J.; O'Keeffe, M.; Yaghi, O.M. Science, 294, 469 (2002).

[6] Klein, N.; Senkovska, I.; Gedrich, K.; Stoeck, U.; Henschel, A.; Mueller, U.; Kaskel, S. Angew. Chem. Int. Ed., 48, 9954 (2009).

[7] Yaghi, O.M.; Davis, C.E.; Li, G.; Li, H. J. Am. Chem. Soc., 119, 2861 (1997).

[8] N. W. Ockwig, O. Delgado-Friedrichs, M. O'Keefe, O. M. Yaghi, Acc. Chem. Res., 38, 176 (2005).

[9] O. M. Yaghi, M. O'Keeffe, N. W. Ockwig, H. K. Chae, M. Eddaoudi, J. Kim, Nature, 423, 705 (2003)

[10] S. Surble, C. Serre, C. Mellot-Draznieks, F. Millange, G. Ferey, Chem. Commun. 2006, 284.

[11] F. P. Doty, C. A. Bauer, A. J. Skulan, P. G. Grant, M. D. Allendorf, "Scintillating Metal-Organic Frameworks: A New Class of Radiation Detection Materials", Advanced Materials, Volume 21, Issue 1, pages 95–101, January 5, (2009).

[12] Donald L. Horrocks "Pulse Shape Discrimination with Organic Liquid Scintillator Solutions", Applied Spectroscopy, 24(4), 397 (1970).

[Blank page following section.]

DISTRIBUTION

Mark Allendorf	8651
Mitchell Anstay	8223
William P. Ballard	8100
Daniel L. Barton	1123
Raghu Bhakta	8651
Janelle Branson	1111
Doug Chinn	1832
Barney Doyle	1111
Bill Even	8650
Patrick Feng	8651
John Goldsmith	8131
Susanna Gordon	8101
Khalid Hattar	1111
Jay Jakubczak	5710
Scott Meek	8651
Curt Nilsen	8130
John Perry	8651
R. Allen Roach	1814
Timothy Shepodd	8223
Michael Smith	1123
Toby Townsend	5717
Andy Vance	8223
Pin Yang	1832
Technical Library	9536 (electronic copy)
D. Chavez,	1011 (LDRD Office)


Sandia National Laboratories